Spontaneous hemolytic uremic syndrome triggered by complement factor H lacking surface recognition domains

Matthew C. Pickering,[1] Elena Goicoechea de Jorge,[3] Rubén Martinez-Barricarte,[3] Sergio Recalde,[4] Alfredo Garcia-Layana,[4] Kirsten L. Rose,[1] Jill Moss,[2] Mark J. Walport,[1] H. Terence Cook,[2] Santiago Rodriguez de Córdoba,[3] and Marina Botto[1]

[1]Molecular Genetics and Rheumatology Section and [2]Department of Histopathology, Faculty of Medicine, Imperial College, London W12 0NN, England, UK
[3]Departamento de Fisiopatologia Celular y Molecular, Centro de Investigaciones Biologicas, Consejo Superior de Investigaciones Científicas and Centro de Investigación Biomédica en Red de Enfermedades Raras–Instituto de Salud Carlos III, 28040 Madrid, Spain
[4]Department of Ophthalmology, University Clinic of Navarra University, 31080 Pamplona, Spain

Factor H (FH) is an abundant serum glycoprotein that regulates the alternative pathway of complement–preventing uncontrolled plasma C3 activation and nonspecific damage to host tissues. Age-related macular degeneration (AMD), atypical hemolytic uremic syndrome (aHUS), and membranoproliferative glomerulonephritis type II (MPGN2) are associated with polymorphisms or mutations in the FH gene (*Cfh*), suggesting the existence of a genotype–phenotype relationship. Although AMD and MPGN2 share pathological similarities with the accumulation of complement-containing debris within the eye and kidney, respectively, aHUS is characterized by renal endothelial injury. This pathological distinction was reflected in our *Cfh* association analysis, which demonstrated that although AMD and MPGN2 share a *Cfh* at-risk haplotype, the haplotype for aHUS was unique. FH-deficient mice have uncontrolled plasma C3 activation and spontaneously develop MPGN2 but not aHUS. We show that these mice, transgenically expressing a mouse FH protein functionally equivalent to aHUS-associated human FH mutants, regulate C3 activation in plasma and spontaneously develop aHUS but not MPGN2. These animals represent the first model of aHUS and provide in vivo evidence that effective plasma C3 regulation and the defective control of complement activation on renal endothelium are the critical events in the molecular pathogenesis of FH-associated aHUS.

CORRESPONDENCE
Matthew Pickering:
matthew.pickering@imperial.ac.uk
OR
Santiago Rodríguez de Córdoba:
SRdeCordoba@cib.csic.es

Factor H (FH) is the major plasma alternative pathway (AP) complement regulator preventing uncontrolled C3 activation and host tissue damage. The association between FH and age-related macular degeneration (AMD) (1), atypical hemolytic uremic syndrome (aHUS) (2–5), and membranoproliferative glomerulonephritis type II (MPGN2) (6–9) supports the hypothesis that AP dysregulation is a unifying pathogenetic feature of these diverse conditions. However, only MPGN2 and AMD have overt pathological similarities. Indeed, AMD-like pathology is well recognized in patients with MPGN2 (10). The hallmark of AMD is drusen, complement-containing material that accumulates beneath the retinal pigmented epithelium, whereas in MPGN2 accumulation of C3 and electron-dense material is seen along the glomerular basement membrane (GBM). In contrast to these "debris-associated" conditions, aHUS is characterized by renal endothelial injury and thrombosis (thrombotic microangiopathy) resulting in hemolytic anemia, thrombocytopenia, and renal failure.

Although complete FH deficiency in humans (6, 8, 9), pigs (11), and mice (12) is associated with reduced C3 and MPGN2, aHUS-associated *CFH* mutations cluster within the carboxy-terminal

M.C. Pickering and E. Goicoechea de Jorge contributed equally to this work.
S. Rodriguez de Córdoba and M. Botto contributed equally to this work.
M.J. Walport's present address is the Wellcome Trust, London NW1 2BE, England, UK.
The online version of this article contains supplemental material.

The Journal of Experimental Medicine

short consensus repeat (SCR) domains of the protein (13), are frequently associated with normal C3 and FH levels, and result in defective binding of FH to heparin, C3b, and endothelium (14–17). Importantly, clustering of these mutations among carboxy-terminal domains would not be expected to alter plasma C3 regulation, because this function resides among the amino-terminal four SCR domains (17, 18). Therefore, we hypothesized that FH-associated aHUS would require both effective plasma C3 regulation and defective regulation on renal endothelium.

RESULTS AND DISCUSSION

That MPGN2 and AMD, but not aHUS, have pathological similarities was recapitulated in the at-risk single nucleotide polymorphism (SNP; Table S1, available at http://www.jem.org/cgi/content/full/jem.20070301/DC1) and haplotype (Fig. 1) association data derived from a comparative genetic analysis, using a minimal set of informative *CFH* SNPs, in Spanish subjects with aHUS, AMD, and MPGN2. No overlapping between *CFH* aHUS-associated at-risk alleles or at-risk haplotypes was seen with the other conditions, consistent with previous data (19, 20). *CFH* haplotype H1 (-332C, c.184G, c.1204C, c.2016A, and c.2808G) was significantly increased in AMD and MPGN2 versus controls but not in aHUS patients. Conversely, haplotype H3 (-332T, c.184G, c.1204T, c.2016G, and c.2808T) was significantly increased in aHUS patients but not in either AMD or MPGN2 patients. Notably, haplotype H2 (-332C, c.184A, c.1204T, c.2016A, and c.2808G), previously shown to protect from AMD (19), was markedly decreased in all three conditions, suggesting that this haplotype may be associated with increased FH regulatory activity and reduced AP activation. A strong correlation between the *CFH* genotypes and the pathological outcome is further supported by the observation that the carboxy-terminal *CFH* mutations, frequently found in aHUS patients (2–5), were not detected in either healthy controls or subjects with MPGN2 or AMD (Table S2). These genetic data support the hypothesis that distinct functional alterations in FH are critical in the pathogenesis of aHUS and AMD/MPGN2.

To test this hypothesis and to establish that a combination of effective plasma C3 regulation and defective regulation on renal endothelium is required for aHUS to develop, we generated transgenic mice expressing a mouse FH protein (FHΔ16-20) that lacked the terminal five SCR domains (Fig. 2 A), the equivalent mouse location of the majority of aHUS-associated FH human mutations (13). These animals were intercrossed with FH-deficient ($Cfh^{-/-}$) mice to generate mice expressing either the mutant protein alone ($Cfh^{-/-}$.FHΔ16-20) or in combination with the full-length mouse protein ($Cfh^{+/-}$.FHΔ16-20). $Cfh^{-/-}$.FHΔ16-20 mice were viable, and FHΔ16-20 was detectable in plasma (Fig. 2 B) at levels comparable to FH in $Cfh^{+/-}$ mice (Fig. 2 C). Analogous to aHUS-associated FH human mutants, FHΔ16-20 retained complement regulatory activity but showed impaired binding to heparin and human umbilical vein endothelial cells (HUVECs) in vitro (Fig. 3).

$Cfh^{-/-}$ mice have secondary plasma C3 depletion (12), enabling us to assess the ability of FHΔ16-20 to regulate AP activation in vivo by measuring C3 levels in the $Cfh^{-/-}$.FHΔ16-20 mice. C3 levels were significantly higher in the

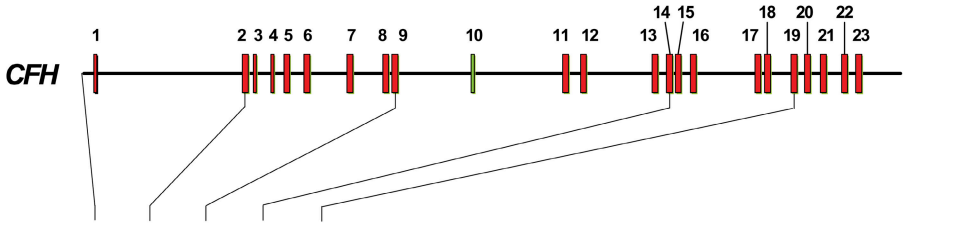

	-332C/T Promoter (rs3753394)	c.184G/A V62I (rs800292)	c.1204T/C Y402H (rs1061170)	c.2016A/G Q672Q (rs3753396)	c.2808G/T E936D (rs1065489)	Control (n=139)	aHUS (n=94)			AMD (n=79)			MPGN2 (n=15)		
						Freq.	Freq.	OR (95% CI)	P value	Freq.	OR (95% CI)	P value	Freq.	OR (95% CI)	P value
H1	C	G	C	A	G	0.228	0.21	-	NS	0.41	2.45 (1.60-3.74)	3×10^{-5}	0.47	2.99 (1.38-6.45)	0.0068
H2	C	A	T	A	G	0.266	0.10	0.30 (0.18-0.53)	$< 10^{-5}$	0.12	0.35 (0.20-0.61)	2×10^{-4}	0.13	0.42 (0.14-1.24)	NS
H3	T	G	T	G	T	0.192	0.31	1.89 (1.23-2.91)	0.0039	0.22	-	NS	0.17	-	NS
H4	C	G	T	A	G	0.167	0.17	-	NS	0.08	0.45 (0.24-0.87)	0.019	0.17	-	NS
H5	T	G	C	A	G	0.075	0.12	-	NS	0.06	-	NS	0.07	-	NS
H6	C	G	T	G	T	0.039	0.02	-	NS	0.05	-	NS	-	-	-

Figure 1. Association analysis of *CFH* haplotypes with aHUS, AMD, and MPGN2 within a single population. Schematic illustration of the *CFH* exon structure demonstrating the location of the five SNPs included in these studies. These SNPs represent a minimal informative set for genetic variation within the *CFH* gene. *CFH* haplotypes with a frequency >3% are shown. The frequency of each *CFH* haplotype was compared with the controls and the aHUS, AMD, and MPGN2 cohorts, and the p-values and the OR were calculated. Risk haplotypes are shaded red, whereas protective haplotypes are shaded in green.p-values were derived using the two-sided Fisher's exact test. OR and 95% confidence interval (95% CI) are shown. See Table S1 for individual *CFH* SNP allele frequencies in patients with these conditions. The nucleotide and amino acid numbering refer to the translation start site (A in ATG is +1; Met is +1), as recommended by the Human Genome Variation Society.

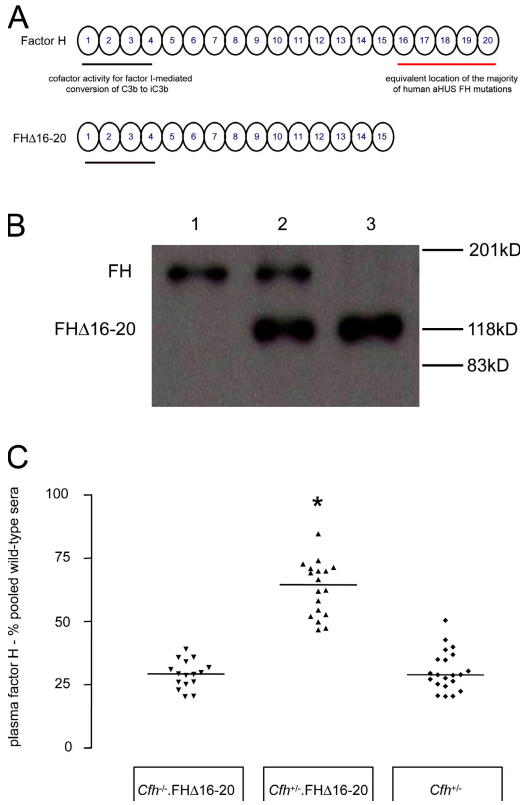

Figure 2. The development of *Cfh*$^{-/-}$.FHΔ16-20 mice. (A) Schematic representation of the mouse FH protein and the mutant mouse FHΔ16-20 protein. SCR domains are numbered incrementally from the amino terminus. Complement regulatory domains are localized within SCR domains 1–4 (black line), whereas the equivalent location of the majority of aHUS-associated human mutations is within SCR domains 16–20 (red line). (B) Western blot of plasma probed with a polyclonal anti–mouse FH antibody from wild-type (lane 1), *Cfh*$^{+/-}$.FHΔ16-20 (lane 2), and *Cfh*$^{-/-}$.FHΔ16-20 mice (lane 3). The truncated mutant FHΔ16-20 protein runs at a lower molecular mass than the 150-kD full-length mouse protein. (C) Plasma FH levels in *Cfh*$^{-/-}$.FHΔ16-20, *Cfh*$^{+/-}$.FHΔ16-20, and *Cfh*$^{+/-}$ mice. Median FHΔ16-20 plasma levels quantified by ELISA in *Cfh*$^{-/-}$.FHΔ16-20 mice were 29.3% pooled wild-type sera (range = 20.1–39.1%; $n = 16$), which were comparable to FH levels in *Cfh*$^{+/-}$ mice (median = 28.9%, range = 20.5–50.5%; $n = 21$; $P > 0.05$). In the *Cfh*$^{+/-}$.FHΔ16-20 mice, total FH levels were 64.5% (range = 46.7–84.6%; $n = 18$), significantly higher than levels in either the *Cfh*$^{-/-}$.FHΔ16-20 ($P < 0.001$) or the *Cfh*$^{+/-}$ ($P < 0.001$) mice. Horizontal bars denote median values. *, $P < 0.001$ for *Cfh*$^{+/-}$.FHΔ16-20 mice versus all other groups using Bonferroni's multiple comparison test.

Cfh$^{-/-}$.FHΔ16-20 mice compared with *Cfh*$^{-/-}$ littermate controls (Fig. 4 A). C3 levels in *Cfh*$^{+/-}$.FHΔ16-20 mice were also significantly higher compared with age-matched *Cfh*$^{+/-}$ mice, reaching wild-type C3 levels (Fig. 4 A). Thus, FHΔ16-20 retained the ability to regulate plasma C3 activation in vivo. Spontaneous GBM C3 deposition is seen in *Cfh*$^{-/-}$ mice (12). To assess the ability of FHΔ16-20 to regulate C3 activation within the kidney, we compared glomerular C3 staining in 3-wk-old *Cfh*$^{-/-}$.FHΔ16-20, *Cfh*$^{+/-}$.FHΔ16-20, and *Cfh*$^{-/-}$ mice (Fig. 4 B). In striking contrast to the linear GBM C3 staining pattern evident in the *Cfh*$^{-/-}$ mice, only a granular mesangial C3 staining pattern was detected in *Cfh*$^{-/-}$.FHΔ16-20 mice. Thus, FHΔ16-20 also efficiently prevented accumulation of C3 along the GBM.

During our initial observations, all *Cfh*$^{-/-}$.FHΔ16-20 mice developed hematuria and anasarca or died before 12 wk of age. Hence, we monitored cohorts of *Cfh*$^{-/-}$.FHΔ16-20 ($n = 15$) and *Cfh*$^{+/-}$.FHΔ16-20 ($n = 11$) mice over an 8-wk period. At 8 wk, 9 out of the 15 *Cfh*$^{-/-}$.FHΔ16-20 mice (60%) had developed hematuria and anasarca, necessitating death, whereas all *Cfh*$^{+/-}$.FHΔ16-20 animals remained well. Renal histology in the *Cfh*$^{-/-}$.FHΔ16-20 mice with hematuria demonstrated thrombotic microangiopathy (Fig. 5 A). Endothelial damage characteristic of thrombotic microangiopathy was evident on ultrastructural examination of these animals (Fig. 5 B). Importantly, electron-dense GBM deposits, an ultrastructural feature of MPGN2 that we have previously shown to be present at this age in *Cfh*$^{-/-}$ mice (12), were absent. No renal histological abnormalities were seen in the 8-wk-old *Cfh*$^{+/-}$.FHΔ16-20 mice, and in a separate cohort of *Cfh*$^{+/-}$.FHΔ16-20 mice ($n = 4$), renal histology remained normal at 6 mo (unpublished data).

In all of the *Cfh*$^{-/-}$.FHΔ16-20 mice with hematuria, there was significant elevation of blood urea (median = 31.8 mmol/liter, range = 26.3–42.8 mmol/liter; $n = 8$) compared with normal values in the age-matched *Cfh*$^{+/-}$.FHΔ16-20 mice (median = 10 mmol/liter, range = 4.8–16.5 mmol/liter; $n = 11$; $P = 0.0003$; Table S3, available at http://www.jem.org/cgi/content/full/jem.20070301/DC1). Red cell fragmentation was evident on the peripheral blood films in all of the *Cfh*$^{-/-}$.FHΔ16-20 mice with hematuria (Fig. 5 C, arrows). Furthermore, these mice had significantly reduced platelet counts (median = 64×10^9 platelets/liter, range = 28–291 platelets/liter; $n = 7$) compared with normal values in the *Cfh*$^{+/-}$.FHΔ16-20 mice (median = 517×10^9 platelets/liter, range = 445–584 platelets/liter; $n = 4$; $P = 0.0061$). Thus, renal thrombotic microangiopathy in *Cfh*$^{-/-}$.FHΔ16-20 mice was associated with renal failure, red cell fragmentation, and thrombocytopenia, all cardinal features of aHUS. Immunofluorescence studies in the *Cfh*$^{-/-}$.FHΔ16-20 mice with hematuria showed C3 deposition along the endothelium and within the smooth muscle of renal arteries (Fig. 5 D, i), in addition to abnormal deposition within the glomerular mesangium and capillary walls (Fig. 5 D, iii). In contrast, no abnormal C3 staining was seen in age-matched *Cfh*$^{+/-}$.FHΔ16-20 mice (Fig. 5 D, ii and iv). Thus, consistent with the in vitro data, FHΔ16-20 failed to regulate C3 activation on renal endothelium.

That a degree of plasma C3 regulation is required to enable thrombotic microangiopathy to develop derived from our observations in a second transgenic line (*Cfh*$^{-/-}$.FHΔ16-20*low*) with a median plasma FHΔ16-20 level of only 2% of normal wild-type FH levels. Median plasma C3 levels were 34.8 mg/liter (range = 20.7–50.1 mg/liter; $n = 6$), significantly less than the median value measured in the *Cfh*$^{-/-}$.FHΔ16-20 mice (79.5 mg/liter; $P < 0.001$) but greater than median C3

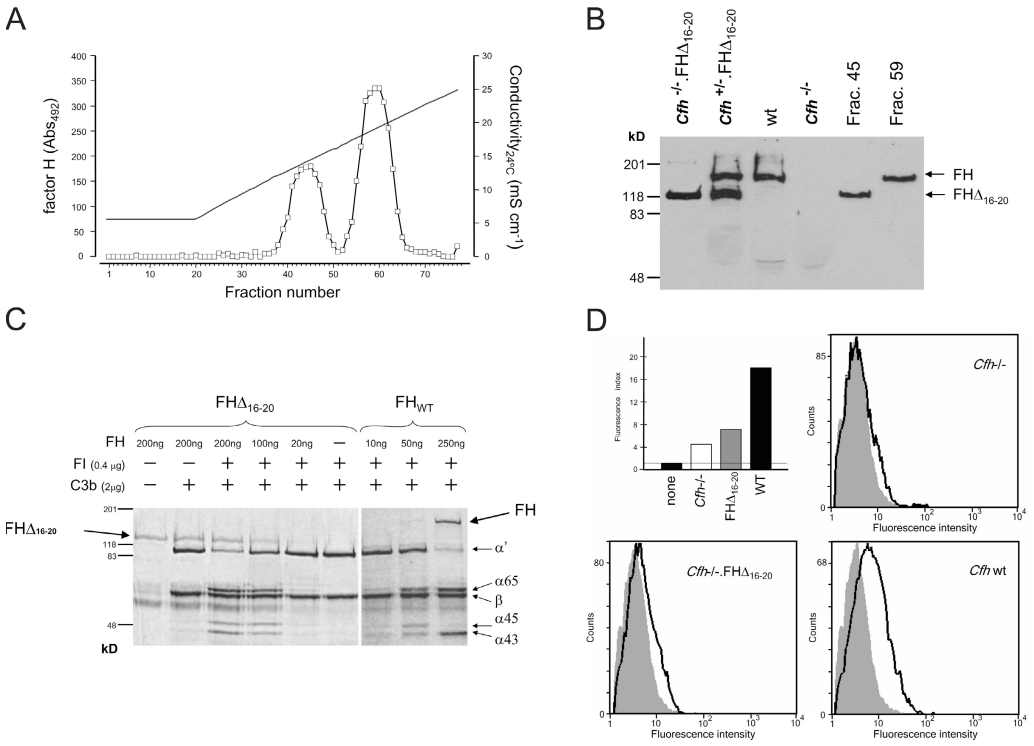

Figure 3. Functional characterization of FHΔ16–20. (A and B) Heparin binding assay. *Cfh*$^{-/+}$.FHΔ16-20 mouse plasma was applied to a heparin–sepharose column, and the proteins bound to the column were eluted with a NaCl linear gradient (35–250 mM). Two protein peaks containing FH identified by ELISA (A) and Western blot analysis (B) showed that the mutant FHΔ16-20 protein eluted before FH, demonstrating that removal of SCR16-20 impairs binding of FH to heparin. The continuous line in A indicates conductivity. (C) Cofactor activity of FHΔ16-20 protein in the proteolysis of fluid-phase mouse C3b by factor I. Different concentrations of either purified FH or FHΔ16-20 protein were incubated with mouse C3b in the presence of factor I. Analysis of C3b proteolytic fragments on 8% SDS-PAGE gel under reducing conditions indicated that both proteins had factor I cofactor activity with the appearance of α chain fragments (α65 and α45/43). Protein fragments were visualized using Coomassie blue staining. (D) HUVEC binding assays (background level indicated by the horizontal line; top left). HUVECs were incubated with 100 μl EDTA plasma dialyzed against 0.5× PBS (137 mM NaCl, 10 mM phosphate, 2.7 mM KCl, pH 7.4). Bound FH or FHΔ16-20 were detected using a rabbit anti–mouse FH antibody and a goat anti–rabbit Alexa Fluor 488–conjugated antibody. Alexa Fluor 488–conjugated isotype-matched antibody was used as a control (shaded area). The fluorescence index was calculated by multiplying the mean fluorescent intensity by the percentage of cells staining positive for FH (bold line). These analyses demonstrated that the mutant FHΔ16-20 protein has a markedly impaired ability to bind to HUVECs in comparison with wild-type protein.

levels in *Cfh*$^{-/-}$ animals (14.3 mg/liter; $P < 0.01$). At 8 mo of age, renal histology in the *Cfh*$^{-/-}$.FHΔ16-20*low* mice ($n = 6$) demonstrated only mild mesangial expansion with no evidence of thrombotic microangiopathy. Furthermore, these mice did not develop hematuria or red cell fragmentation, and serum urea levels remained normal at the time of death (median = 10.6 mmol/liter, range = 8.9–11.5 mmol/liter). Capillary wall C3 staining was reduced in comparison to age-matched *Cfh*$^{-/-}$ mice, and subendothelial electron-dense GBM deposits were infrequent. Hence, the plasma C3 regulation in the *Cfh*$^{-/-}$.FHΔ16-20*low* mice was insufficient for aHUS to develop but did prevent the development of MPGN2 up to the time point examined. The data from both transgenic lines, together with the observation that aHUS did not develop in *Cfh*$^{-/-}$ mice that have secondary C3 depletion, demonstrated that C3 activation is a key effector mechanism in aHUS.

There is now overwhelming evidence that aHUS is associated with defective regulation of the AP of complement activation. Mutations affecting the cofactors for the factor I–mediated proteolytic inactivation of activated C3 in plasma (FH; references 2–5, 21) and on cell surfaces (membrane cofactor protein; references 15, 22), in addition to mutations affecting the serine protease factor I itself (23), predispose to the development of aHUS. Similarly, gain-of-function mutations in the complement activator factor B also predispose to aHUS, further supporting the critical role of C3 activation in the pathogenesis of aHUS (24). The spontaneous pathology in the *Cfh*$^{-/-}$.FHΔ16-20 mice, like that of humans with functionally similar FH mutations, targeted the renal vasculature, suggesting that there are unique anatomical and/or physiological properties of this endothelial bed that render it particularly sensitive to complement-mediated damage.

Interestingly, aHUS-associated mutations in complement genes are normally found in heterozygosis in aHUS patients and are frequently associated with incomplete penetrance. In this respect, it is notable that *Cfh*$^{+/-}$.FHΔ16-20 mice did not

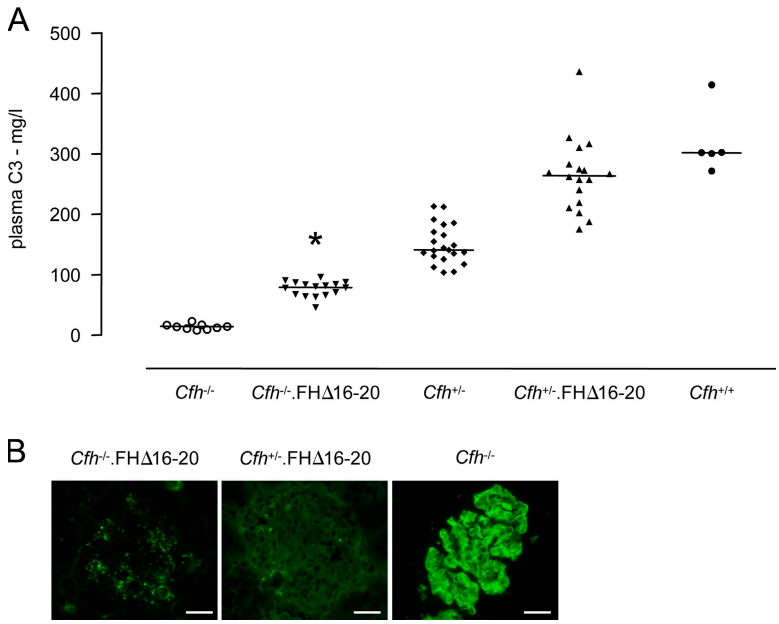

Figure 4. Plasma and glomerular C3 regulation in *Cfh*$^{-/-}$.FHΔ16–20 mice. (A) Plasma C3 levels in *Cfh*$^{-/-}$.FHΔ16-20 mice. Median plasma C3 levels in the *Cfh*$^{-/-}$.FHΔ16-20 mice were 79.5 mg/liter (range = 46.1–95.9 mg/liter; $n = 16$), which was significantly higher than the levels seen in the *Cfh*$^{-/-}$ mice (median = 14.3 mg/liter, range = 7.9–23.2 mg/liter; $n = 9$; $P < 0.05$). C3 levels were also significantly higher in the *Cfh*$^{+/-}$.FHΔ16-20 mice compared with *Cfh*$^{+/-}$ mice (medians = 264.6 vs. 142 mg/liter, respectively; $P < 0.001$) and did not differ from the levels seen in wild-type animals. Horizontal bars denote median values. *, $P < 0.05$ for *Cfh*$^{-/-}$.FHΔ16-20 mice versus all other groups using Bonferroni's multiple comparison test. (B) Glomerular C3 staining in 3-wk-old *Cfh*$^{-/-}$.FHΔ16-20, *Cfh*$^{+/-}$.FHΔ16-20, and *Cfh*$^{-/-}$ mice. The striking GBM linear C3 staining pattern seen in the glomeruli of the *Cfh*$^{-/-}$ mice was not evident in either *Cfh*$^{-/-}$.FHΔ16-20 or *Cfh*$^{+/-}$.FHΔ16-20 mice, consistent with the ability of FHΔ16-20 to prevent GBM C3 deposition. Although no staining was detected in the glomeruli of *Cfh*$^{+/-}$.FHΔ16-20 animals, a granular mesangial C3 staining pattern was evident in *Cfh*$^{-/-}$.FHΔ16-20 mice. Bar, 10 μm.

spontaneously develop aHUS, suggesting that, like in some human patients, multiple genetic defects affecting complement regulators are required for aHUS to develop in mice (25, 26). Furthermore, infection, immunosuppressive drugs, cancer therapies, oral contraceptive agents, pregnancy, or postpartum period are all factors that may trigger aHUS in individuals carrying *CFH* mutations in heterozygosis, and the syndrome has developed in the native kidney of live-related kidney donors who had previously unidentified FH mutations (27). Thus, *Cfh*$^{+/-}$.FHΔ16-20 mice may only develop aHUS after an additional insult, either genetic or environmental (or both), although interspecies differences in the regulation of C3 on cell surfaces by FH and other complement regulators may also be relevant to the apparent resistance of *Cfh*$^{+/-}$.FHΔ16-20 mice to aHUS.

Treatment of aHUS associated with FH mutations is difficult. Renal transplantation is associated with a high incidence of disease recurrence (28). Plasma infusions as a source of FH have been beneficial (29) but can result in hyperproteinemia, requiring plasma exchange (30). The principle source of FH is hepatic, and hence, the expected definitive treatment would be combined liver and renal transplantation, which has produced mixed results (31–33). Our data define an important aspect of therapy. Agents that attempt to restore C3 regulation must critically achieve this on cell surfaces. Indeed, our observations suggest that restoration of fluid-phase regulation alone may, by increasing the circulating plasma C3 levels, be deleterious.

In conclusion, the similarities between the surface recognition domains of mouse and human FH (34) enabled us to mutate mouse FH to functionally mimic aHUS-associated human FH mutations. *Cfh*$^{-/-}$ mice expressing this mutant FH protein spontaneously developed aHUS, not MPGN2. Our data provide the first in vivo proof of principle evidence that FH mutations specifically impairing surface recognition can result in spontaneous aHUS and define the molecular pathogenesis of aHUS-associated FH mutations.

MATERIALS AND METHODS

Patients. This study included three independent cohorts of Spanish patients, comprising 94 aHUS patients selected on the basis of a clinical history of HUS with nondiarrhea-associated origin, 79 patients >60 yr old with AMD who presented with advanced choroidal neovascularization and drusen in both eyes, and 15 MPGN2 patients. An independent cohort of 139 age-matched healthy Spanish controls with no family history of AMD, aHUS, or MPGN2 was also used in these experiments. Genomic DNA was generated from peripheral blood leukocytes using standard procedures. All protocols included in these studies have been approved by national and/or local institutional review boards, and all subjects gave their informed consent.

Genotyping and statistical analyses. A set of five SNPs, representing a minimal informative set for genetic variation within the *CFH* gene, were genotyped in controls and in the aHUS, AMD, and MPGN2 cohorts on genomic DNA by allelic discrimination using probes (TaqMan; Applied Biosystems)

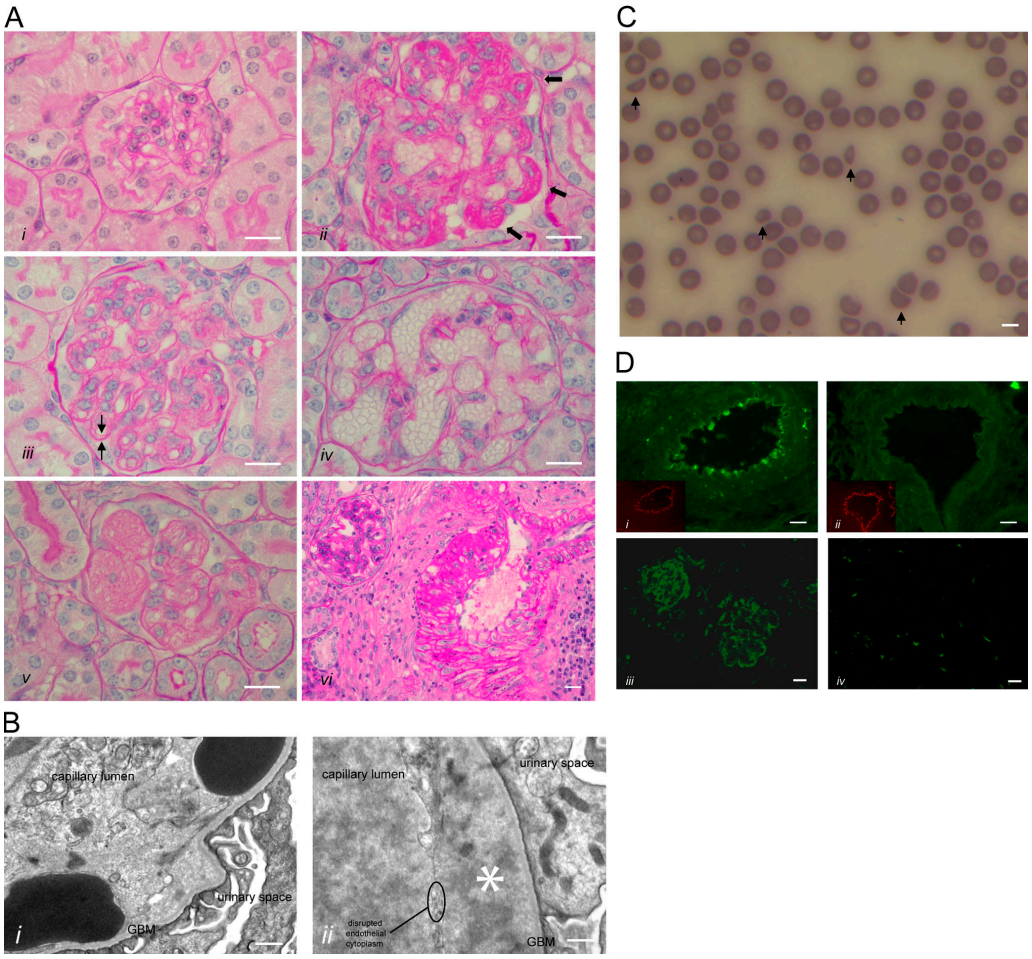

Figure 5. HUS in *Cfh*$^{-/-}$.FHΔ16–20 mice. (A) Renal histology in *Cfh*$^{-/-}$.FHΔ16-20 mice. Normal glomerulus from a 2-mo-old *Cfh*$^{+/-}$. FHΔ16-20 mouse (i), and light microscopic features of thrombotic microangiopathy in *Cfh*$^{-/-}$.FHΔ16-20 mice (ii–vi). These included glomerular microthrombi (ii, arrows), capillary wall double contours (iii, arrows), formation of capillary microaneurysms (iv), and mesangiolysis (v). Inflammatory changes were also seen within glomerular arteries (vi). Bar, 10 μm. (B) Electron microscopy revealed characteristic ultrastructural changes of thrombotic microangiopathy. Erythrocytes beneath disrupted endothelium and in direct contact with the GBM (i) and endothelial disruption with subendothelial accumulation of flocculent material (ii, asterisk). Note the absence of GBM electron-dense deposits, an ultrastructural feature of MPGN2 that is normally evident at this age in *Cfh*$^{-/-}$ mice (reference 12). Bar, 500 nm. (C) Peripheral blood smear from a *Cfh*$^{-/-}$.FHΔ16-20 mouse with hematuria. Evidence of red-cell fragmentation is seen (arrows). Bar, 5 μm. (D) Renal C3 staining. C3 deposition along the endothelium and within the smooth muscle of renal arteries was present in the *Cfh*$^{-/-}$. FHΔ16-20 (i) but not the *Cfh*$^{+/-}$.FHΔ16-20 (ii) mice. Insets represent the staining of mouse endothelium with anti-CD31 (platelet/endothelial cell adhesion molecule). Mesangial and capillary wall C3 staining in a *Cfh*$^{-/-}$. FHΔ16-20 mouse with HUS (iii) in contrast to an absence of abnormal glomerular C3 staining in an age-matched *Cfh*$^{+/-}$.FHΔ16-20 mouse (iv). No abnormal renal IgG staining was present in either the *Cfh*$^{-/-}$.FHΔ16-20 or the *Cfh*$^{+/-}$.FHΔ16-20 mice (not depicted). Bar, 10 μm.

and real-time PCR equipment (PE7700; Applied Biosystems), according to the manufacturer's specifications, or by automatic DNA sequencing of PCR-derived amplicons in a sequencer (ABI 3730; Applied Biosystems) using a dye terminator cycle sequencing kit (Applied Biosystems). Sequences of *CFH* exons 22 and 23 were determined in all individual controls and patients using PCR-derived amplicons, as previously described (26). The frequency of alleles 1 and 2 from each SNP was compared with controls and aHUS, AMD, and MPGN2 cohorts, and the p- values, odds ratios (ORs), and 95% confidence intervals were calculated. Haplotype frequencies in the control and patient cohorts were estimated using the expectation maximization algorithm implemented by the SNPStats software (available at http://bioinfo.iconcologia.net/SNPstats). Nonparametric data were given as the median, with the range of values in parentheses, as indicated in the figures. We used the Mann-Whitney test to compare two groups and Bonferroni's multiple comparison test for the analysis of three groups. Data were analyzed by Prism software (version 3.00 for Windows; GraphPad Software).

Mice. Cfh$^{-/-}$ mice were generated as previously described (12). To generate the FHΔ16-20 protein, the codon encoding Cys937 at the beginning of SCR16 of mouse FH was substituted by a stop codon in the full-length cDNA clone using site-directed mutagenesis (QuickChange; Stratagene). A modified version of the pCAGGS plasmid (35) bearing the CMV-EI enhancer, the chicken β-actin promoter, and intron 1 and the simian virus 40 poly(A) signal was used to construct the FHΔ16-20–encoding transgene. The construct was excised from the vector by digestion with Kpn I and Sal I and purified using a gel extraction kit (QIAEX II; QIAGEN), followed by Elutip purification (Schleicher and Schuell). The DNA was injected into fertilized CBA × C57BL/6 F1 mouse eggs, and these were transplanted into

foster females. Progeny were screened for transgene integration by PCR, and expression of the mutant FH protein was determined by Western blotting. Heterozygous and homozygous FH-deficient mice expressing the transgene were generated by intercrossing the transgenic animals with $Cfh^{-/-}$ mice. The presence of the transgene was detected by PCR using genomic DNA and oligonucleotides located within exon 5 (mHF1-4F, 5′-GCAATTCAGGCTTCAAGATTG-3′), exon 9 (mHF1-8F, 5′-GACATGTACAGAGAATGGCTG-3′), and exon 13 (mHF1-6R, 5′-CCCATTAAGAATTTCAAGAGGTG-3′) of the mouse FH exonic sequence. The genotyping of the $Cfh^{-/-}$ mouse has been previously described (12). All animal procedures were done in accordance with institutional guidelines.

Measurement of FH and C3 levels and Western blotting of plasma FH. FH levels were measured by ELISA using a goat anti–rat FH antibody (a gift from M. Daha, Leiden University Medical Center, Leiden, Netherlands) and a rabbit anti–mouse FH antibody. Samples were quantified by reference to a standard curve generated using normal wild-type mouse serum. C3 levels were measured by ELISA using a goat anti–mouse C3 antibody (MP Biomedicals). Results were quantified by reference to a standard curve generated from acute-phase sera containing a known quantity of C3 (Calbiochem). Mouse FH was detected by the Western blotting of serum with a cross-reactive polyclonal rabbit antibody against rat FH.

Heparin binding assay and cofactor activity. 200 μl EDTA plasma from a $Cfh^{-/+}$.FHΔ16-20 mouse was dialyzed against 20 mM Tris-HCl (pH 7.4), 35 mM NaCl and applied to a heparin–sepharose column (HiTrap Heparin HP; GE Healthcare). After extensive washes, the proteins bound to the column were eluted with a NaCl linear gradient (35–250 mM). Two protein peaks containing FH were identified by ELISA, and the eluted FH proteins were characterized by Western blot analysis. For the cofactor assay, we thank R.B. Sim (University of Oxford, Oxford, UK) for providing purified human factor I.

Histological studies. For light microscopy, kidneys were fixed in Bouin's solution and embedded in paraffin, and sections were stained with periodic acid Schiff reagent. For immunofluorescence studies, kidneys were snap frozen. FITC-conjugated goat antibody against mouse C3 (MP Biomedicals) and FITC-conjugated goat antibody against mouse IgG (Sigma-Aldrich) were used on snap-frozen sections. Mouse endothelium was stained using a rat anti–mouse CD31 (platelet/endothelial cell adhesion molecule 1) antibody (a gift from B. Imhof, University of Geneva, Geneva, Switzerland), followed by application of Texas red goat polyclonal anti–rat IgG antibody (Abcam). For electron microscopy, samples were fixed in 3% glutaraldehyde, postfixed in 2% aqueous osmium tetroxide, and embedded in Spurr's resin. Ultrathin sections were stained with 1% aqueous uranyl acetate and Reynold's lead citrate.

Assessment of renal function and hematological parameters. We measured serum urea using a UV method kit (R-Biopharm Rhone Ltd.) according to the manufacturer's instructions. Urinalysis was performed using Hema-Combistix (Bayer). Platelets were quantified manually. In brief, whole blood was diluted 1:20 with 1% ammonium oxalate, and the suspension was mixed for 15 min to allow red cell lysis to occur. Samples were transferred to a hemocytometer (Bright-Line; Sigma-Aldrich), and platelets were directly counted. Blood films were manually prepared using EDTA whole blood and stained using a rapid staining kit (Diff-Quik; Dade Behring).

Online supplemental material. Table S1 shows the frequencies of *CFH* polymorphisms in individuals with MPGN2, aHUS, and AMD. Table S2 shows the frequency of mutations in *CFH* exons 22 and 23 in controls and individuals with MPGN2, aHUS, and AMD. Table S3 shows mortality, renal function, and hematological parameters in $Cfh^{-/-}$.FHΔ16-20 and $Cfh^{+/-}$.FHΔ16-20 mice. Online supplemental material is available at http://www.jem.org/cgi/content/full/jem.20070301/DC1.

We are grateful to all patients and the collaborating clinicians for their participation in this study. We thank Mr. Ian Shore for his technical assistance with the preparation of tissue for electron microscopy, Mrs. Margarita Lewis for technical assistance with the processing of histological specimens, and the staff of the Biological Services Unit at Imperial College for the care of the animals involved in this study. We also thank the members of the DNA sequencing laboratory at the Centro de Investigaciones Biologicas, as well as Dr. Elena Aller and Ms. Sheila Pinto for invaluable technical assistance with patient genotyping.

These studies were funded by the Wellcome Trust and the Spanish Ministerio de Educación y Cultura (grant SAF2005-00913). M.C. Pickering is a Wellcome Trust Research Fellow (fellowship GR071390).

The authors have no conflicting financial interests.

Submitted: 8 February 2007
Accepted: 13 April 2007

REFERENCES

1. Scholl, H.P., M. Fleckenstein, P.C. Issa, C. Keilhauer, F.G. Holz, and B.H. Weber. 2007. An update on the genetics of age-related macular degeneration. *Mol. Vis.* 13:196–205.
2. Caprioli, J., P. Bettinaglio, P.F. Zipfel, B. Amadei, E. Daina, S. Gamba, C. Skerka, N. Marziliano, G. Remuzzi, and M. Noris. 2001. The molecular basis of familial hemolytic uremic syndrome: mutation analysis of factor H gene reveals a hot spot in short consensus repeat 20. *J. Am. Soc. Nephrol.* 12:297–307.
3. Perez-Caballero, D., C. Gonzalez-Rubio, M.E. Gallardo, M. Vera, M. Lopez-Trascasa, S. Rodriguez de Cordoba, and P. Sanchez-Corral. 2001. Clustering of missense mutations in the C-terminal region of factor H in atypical hemolytic uremic syndrome. *Am. J. Hum. Genet.* 68:478–484.
4. Richards, A., M.R. Buddles, R.L. Donne, B.S. Kaplan, E. Kirk, M.C. Venning, C.L. Tielemans, J.A. Goodship, and T.H. Goodship. 2001. Factor H mutations in hemolytic uremic syndrome cluster in exons 18-20, a domain important for host cell recognition. *Am. J. Hum. Genet.* 68:485–490.
5. Warwicker, P., T.H. Goodship, R.L. Donne, Y. Pirson, A. Nicholls, R.M. Ward, P. Turnpenny, and J.A. Goodship. 1998. Genetic studies into inherited and sporadic hemolytic uremic syndrome. *Kidney Int.* 53:836–844.
6. Lopez-Larrea, C., M.A. Dieguez, A. Enguix, O. Dominguez, B. Marin, and E. Gomez. 1987. A familial deficiency of complement factor H. *Biochem. Soc. Trans.* 15:648–649.
7. Licht, C., S. Heinen, M. Jozsi, I. Loschmann, R.E. Saunders, S.J. Perkins, R. Waldherr, C. Skerka, M. Kirschfink, B. Hoppe, and P.F. Zipfel. 2006. Deletion of Lys224 in regulatory domain 4 of Factor H reveals a novel pathomechanism for dense deposit disease (MPGN II). *Kidney Int.* 70:42–50.
8. Levy, M., L. Halbwachs-Mecarelli, M.C. Gubler, G. Kohout, A. Bensenouci, P. Niaudet, G. Hauptmann, and P. Lesavre. 1986. H deficiency in two brothers with atypical dense intramembranous deposit disease. *Kidney Int.* 30:949–956.
9. Dragon-Durey, M.A., V. Fremeaux-Bacchi, C. Loirat, J. Blouin, P. Niaudet, G. Deschenes, P. Coppo, W. Herman Fridman, and L. Weiss. 2004. Heterozygous and homozygous factor h deficiencies associated with hemolytic uremic syndrome or membranoproliferative glomerulonephritis: report and genetic analysis of 16 cases. *J. Am. Soc. Nephrol.* 15:787–795.
10. Mullins, R.F., N. Aptsiauri, and G.S. Hageman. 2001. Structure and composition of drusen associated with glomerulonephritis: implications for the role of complement activation in drusen biogenesis. *Eye.* 15:390–395.
11. Hogasen, K., J.H. Jansen, T.E. Mollnes, J. Hovdenes, and M. Harboe. 1995. Hereditary porcine membranoproliferative glomerulonephritis type II is caused by factor H deficiency. *J. Clin. Invest.* 95:1054–1061.
12. Pickering, M.C., H.T. Cook, J. Warren, A.E. Bygrave, J. Moss, M.J. Walport, and M. Botto. 2002. Uncontrolled C3 activation causes membranoproliferative glomerulonephritis in mice deficient in complement factor H. *Nat. Genet.* 31:424–428.
13. Rodriguez de Cordoba, S., J. Esparza-Gordillo, E. Goicoechea de Jorge, M. Lopez-Trascasa, and P. Sanchez-Corral. 2004. The human complement factor H: functional roles, genetic variations and disease associations. *Mol. Immunol.* 41:355–367.

14. Manuelian, T., J. Hellwage, S. Meri, J. Caprioli, M. Noris, S. Heinen, M. Jozsi, H.P. Neumann, G. Remuzzi, and P.F. Zipfel. 2003. Mutations in factor H reduce binding affinity to C3b and heparin and surface attachment to endothelial cells in hemolytic uremic syndrome. *J. Clin. Invest.* 111:1181–1190.
15. Noris, M., S. Brioschi, J. Caprioli, M. Todeschini, E. Bresin, F. Porrati, S. Gamba, and G. Remuzzi. 2003. Familial haemolytic uraemic syndrome and an MCP mutation. *Lancet.* 362:1542–1547.
16. Sanchez-Corral, P., C. Gonzalez-Rubio, S. Rodriguez de Cordoba, and M. Lopez-Trascasa. 2004. Functional analysis in serum from atypical Hemolytic Uremic Syndrome patients reveals impaired protection of host cells associated with mutations in factor H. *Mol. Immunol.* 41:81–84.
17. Sanchez-Corral, P., D. Perez-Caballero, O. Huarte, A.M. Simckes, E. Goicoechea, M. Lopez-Trascasa, and S.R. de Cordoba. 2002. Structural and functional characterization of factor H mutations associated with atypical hemolytic uremic syndrome. *Am. J. Hum. Genet.* 71:1285–1295.
18. Sharma, A.K., and M.K. Pangburn. 1996. Identification of three physically and functionally distinct binding sites for C3b in human complement factor H by deletion mutagenesis. *Proc. Natl. Acad. Sci. USA.* 93:10996–11001.
19. Hageman, G.S., D.H. Anderson, L.V. Johnson, L.S. Hancox, A.J. Taiber, L.I. Hardisty, J.L. Hageman, H.A. Stockman, J.D. Borchardt, K.M. Gehrs, et al. 2005. A common haplotype in the complement regulatory gene factor H (HF1/CFH) predisposes individuals to age-related macular degeneration. *Proc. Natl. Acad. Sci. USA.* 102:7227–7232.
20. Caprioli, J., F. Castelletti, S. Bucchioni, P. Bettinaglio, E. Bresin, G. Pianetti, S. Gamba, S. Brioschi, E. Daina, G. Remuzzi, and M. Noris. 2003. Complement factor H mutations and gene polymorphisms in haemolytic uraemic syndrome: the C-257T, the A2089G and the G2881T polymorphisms are strongly associated with the disease. *Hum. Mol. Genet.* 12:3385–3395.
21. Neumann, H.P., M. Salzmann, B. Bohnert-Iwan, T. Mannuelian, C. Skerka, D. Lenk, B.U. Bender, M. Cybulla, P. Riegler, A. Konigsrainer, et al. 2003. Haemolytic uraemic syndrome and mutations of the factor H gene: a registry-based study of German speaking countries. *J. Med. Genet.* 40:676–681.
22. Richards, A., E.J. Kemp, M.K. Liszewski, J.A. Goodship, A.K. Lampe, R. Decorte, M.H. Muslumanoglu, S. Kavukcu, G. Filler, Y. Pirson, et al. 2003. Mutations in human complement regulator, membrane cofactor protein (CD46), predispose to development of familial hemolytic uremic syndrome. *Proc. Natl. Acad. Sci. USA.* 100:12966–12971.
23. Fremeaux-Bacchi, V., M.A. Dragon-Durey, J. Blouin, C. Vigneau, D. Kuypers, B. Boudailliez, C. Loirat, E. Rondeau, and W.H. Fridman. 2004. Complement factor I: a susceptibility gene for atypical haemolytic uraemic syndrome. *J. Med. Genet.* 41:e84.
24. Goicoechea de Jorge, E., C.L. Harris, J. Esparza-Gordillo, L. Carreras, E.A. Arranz, C.A. Garrido, M. Lopez-Trascasa, P. Sanchez-Corral, B.P. Morgan, and S. Rodriguez de Cordoba. 2007. Gain-of-function mutations in complement factor B are associated with atypical hemolytic uremic syndrome. *Proc. Natl. Acad. Sci. USA.* 104:240–245.
25. Esparza-Gordillo, J., E.G. Jorge, C.A. Garrido, L. Carreras, M. Lopez-Trascasa, P. Sanchez-Corral, and S.R. de Cordoba. 2006. Insights into hemolytic uremic syndrome: segregation of three independent predisposition factors in a large, multiple affected pedigree. *Mol. Immunol.* 43:1769–1775.
26. Esparza-Gordillo, J., E. Goicoechea de Jorge, A. Buil, L. Carreras Berges, M. Lopez-Trascasa, P. Sanchez-Corral, and S. Rodriguez de Cordoba. 2005. Predisposition to atypical hemolytic uremic syndrome involves the concurrence of different susceptibility alleles in the regulators of complement activation gene cluster in 1q32. *Hum. Mol. Genet.* 14:703–712.
27. Donne, R.L., I. Abbs, P. Barany, C.G. Elinder, M. Little, P. Conlon, and T.H. Goodship. 2002. Recurrence of hemolytic uremic syndrome after live related renal transplantation associated with subsequent de novo disease in the donor. *Am. J. Kidney Dis.* 40:E22.
28. Loirat, C., and P. Niaudet. 2003. The risk of recurrence of hemolytic uremic syndrome after renal transplantation in children. *Pediatr. Nephrol.* 18:1095–1101.
29. Licht, C., A. Weyersberg, S. Heinen, L. Stapenhorst, J. Devenge, B. Beck, R. Waldherr, M. Kirschfink, P.F. Zipfel, and B. Hoppe. 2005. Successful plasma therapy for atypical hemolytic uremic syndrome caused by factor H deficiency owing to a novel mutation in the complement cofactor protein domain 15. *Am. J. Kidney Dis.* 45:415–421.
30. Filler, G., S. Radhakrishnan, L. Strain, A. Hill, G. Knoll, and T.H. Goodship. 2004. Challenges in the management of infantile factor H associated hemolytic uremic syndrome. *Pediatr. Nephrol.* 19:908–911.
31. Cheong, H.I., B.S. Lee, H.G. Kang, H. Hahn, K.S. Suh, I.S. Ha, and Y. Choi. 2004. Attempted treatment of factor H deficiency by liver transplantation. *Pediatr. Nephrol.* 19:454–458.
32. Remuzzi, G., P. Ruggenenti, D. Codazzi, M. Noris, J. Caprioli, G. Locatelli, and B. Gridelli. 2002. Combined kidney and liver transplantation for familial haemolytic uraemic syndrome. *Lancet.* 359:1671–1672.
33. Saland, J.M., S.H. Emre, B.L. Shneider, C. Benchimol, S. Ames, J.S. Bromberg, G. Remuzzi, L. Strain, and T.H. Goodship. 2006. Favorable long-term outcome after liver-kidney transplant for recurrent hemolytic uremic syndrome associated with a factor H mutation. *Am. J. Transplant.* 6:1948–1952.
34. Cheng, Z.Z., J. Hellwage, H. Seeberger, P.F. Zipfel, S. Meri, and T.S. Jokiranta. 2006. Comparison of surface recognition and C3b binding properties of mouse and human complement factor H. *Mol. Immunol.* 43:972–979.
35. Shimizu, S., M. Narita, and Y. Tsujimoto. 1999. Bcl-2 family proteins regulate the release of apoptogenic cytochrome c by the mitochondrial channel VDAC. *Nature.* 399:483–487.